Optical absorption and Photoluminescence studies of Erbium doped nanocrystalline CaF2

Venkata Reddy. G. N.
Assistant Professor, Department of Physics, HPPC Government First Grade College, Challakere – 577522, Karnataka, India, Email - gnvr77@gmail.com

Abstract

Erbium (Er^{3+}) doped nanocrystalline calcium fluoride (CaF_2) has been investigated for its optical absorption and photoluminescence (PL) properties due to its relevance in photonic and up conversion applications. Nano crystalline CaF_2:Er^{3+} samples were synthesized and characterized to study the influence of Er^{3+} ion incorporation and Nano scale effects on their optical behaviour. The optical absorption spectra exhibit well- defined 4f–4f transitions of Er^{3+} ions from the ground state $^4I_{15/2}$ to higher excited states, with slight broadening attributed to crystal field variations in the nanocrystalline matrix. Photoluminescence measurements under UV– visible excitation reveal strong green emissions corresponding to the $^2H_{11/2} \rightarrow {}^4I_{15/2}$ and $^4S_{3/2} \rightarrow {}^4I_{15/2}$ transitions, along with red emission from the $^4F_{9/2} \rightarrow {}^4I_{15/2}$ level. The prominent near-infrared emission around 1.53 μm, arising from the $^4I_{13/2} \rightarrow {}^4I_{15/2}$ transition, confirms the suitability of CaF_2 as a low-phonon-energy host for Er^{3+}- based optical devices. The results demonstrate that nanocrystallinity enhances spectral broadening, modifies local symmetry around Er^{3+} ions, and influences emission intensity through surface-related quenching effects. These findings highlight the potential of Er^{3+}-doped CaF_2 nanocrystals for applications in optical amplifiers, up conversion phosphors, and photonic materials.

Keywords: calcium fluoride; phosphors; Photoluminescence; transition; photonic materials;

1. Introduction:-

Rare-earth (RE) ion–doped inorganic materials have been the subject of extensive research in solid-state lighting, lasers, optical amplifiers, and photonic devices due to their unique optical characteristics arising from the shielding of 4f-electrons by outer 5s and 5p orbitals. Among RE ions, erbium (Er^{3+}) occupies a central place because of its technologically important intra-4f transitions, especially the $^4I_{13/2} \rightarrow {}^4I_{15/2}$ transition near 1.53 μm**,** which lies in the third telecommunication window and forms the basis of erbium-doped fiber amplifiers (EDFA) used in optical communication systems [1]. Er^{3+} also exhibits visible emissions in the green and red regions due to transitions within the $^2H_{11/2}$, $^4S_{3/2}$, and $^4F_{9/2}$ levels, enabling applications in up conversion devices, displays, and sensors [2]. Calcium fluoride (CaF_2) is an excellent host matrix for rare-earth ions due to its Cubic fluorite structure (Fm_3m) with high symmetry, Wide band gap (~12 eV), ensuring transparency from UV to IR, Low phonon energy (~470 cm^{-1})**,** significantly suppressing multi-phonon relaxation, Chemical and thermal stability and Ability to accommodate trivalent lanthanide ions with charge compensation via interstitial fluoride ions. The low phonon energy is particularly crucial, it minimizes non- radiative losses and enhances the radiative efficiency of Er^{3+} emission [3]. Therefore, CaF_2 is well regarded as a promising host for efficient up conversion and down conversion processes.

At the nanoscale, slight variations in local symmetry, lattice strain, or distortions around the Er^{3+} ions can cause, Broadening of absorption bands, Shifts in peak positions and Modified crystal-field splitting. Such spectral inhomogeneity is not prominent in bulk CaF_2 but becomes significant in nanocrystalline samples. High surface-to-volume ratios lead to, Increased density of defects, dangling bonds, and surface states, Enhanced probability of non-radiative relaxation and Influence on charge-compensation mechanisms. Surface defects may act as luminescence quenchers, particularly affecting the green up conversion bands of Er^{3+} [4]. Nanocrystalline CaF_2 can contain intrinsic defects such as, Fluoride vacancies, interstitial fluorine (F^-) ions and F-centers (electron trapped at an anion vacancy). These defects may interact with Er^{3+} ions, affecting optical absorption and influencing luminescence pathways.

Optical absorption spectroscopy is essential to study the electronic transitions of Er^{3+} from the ground state $^4I_{15/2}$ to higher excited states such as $^4I_{11/2}$, $^4I_{9/2}$, $^4F_{9/2}$, $^4F_{7/2}$, $^2H_{11/2}$, and others. These transitions appear as sharp, well-defined peaks because 4f electrons are shielded. In nanocrystalline CaF_2, absorption spectra often reveal, Broader features due to inhomogeneous broadening, Changes in oscillator strengths due to modified site symmetry and Additional absorption bands linked to radiation-induced or synthesis-related defects. When doping concentration increases, absorption intensity initially grows but excessive Er^{3+} content can lead to ion clustering and concentration quenching. Photoluminescence (PL) studies provide direct information about the radiative relaxation processes of Er^{3+} ions. Under UV or visible excitation, emissions typically arise from Green bands, $^2H_{11/2} \rightarrow {}^4I_{15/2}$ (~520–530 nm) , $^4S_{3/2} \rightarrow {}^4I_{15/2}$ (~540–560 nm), Red band, $^4F_{9/2} \rightarrow {}^4I_{15/2}$ (~650–670 nm),

Near-IR emission, $^4I_{13/2} \rightarrow {}^4I_{15/2}$ (~1530 nm). CaF_2's low phonon energy favors strong green and red emissions, and the IR transition becomes highly efficient and long-lived. When pumped at ~980 nm, Er^{3+}-doped CaF_2 can exhibit efficient up conversion because, Non-radiative losses are minimal, Energy transfer upconversion (ETU) is facilitated and Cross-relaxation processes are manageable, especially at moderate doping concentrations. In nanocrystals, however, surface-related quenching may weaken upconversion unless surface passivation or core–shell structures are used [5 – 6].

Studying optical absorption and photoluminescence in Er^{3+}-doped nanocrystalline CaF_2 is crucial because, Understanding Local Structure, OA and PL spectra provide insight into the Er^{3+} site symmetry, charge compensation mechanisms, and defect interactions. Optimizing Doping Concentration Identifying the optimum Er^{3+} concentration is necessary to minimize concentration quenching while maximizing luminescence. Exploring Up conversion Mechanisms, PL and power-dependence studies reveal the multiphoton processes and energy-transfer dynamics. Engineering Material for Applications, Improved understanding guides the design of materials for, Fiber amplifiers, NIR emitters, Biolabels and bioimaging, Sensors, Solid-state lasers, Colour displays, Solar converters, Studying the Effects of Nanostructuring Size reduction introduces new optical behaviors, making systematic spectroscopic study essential [7 – 8].

The present research focuses on Synthesis of Er^{3+}-doped CaF_2 nanocrystals using controlled wet-chemical routes. Structural characterization to determine crystallinity, phase purity, and particle size. Detailed optical absorption studies of Er^{3+} intra-4f transitions. Photoluminescence (PL) analysis under various excitation wavelengths. Investigation of energy-transfer mechanisms, defect participation, and quenching effects. Such a study enhances the understanding of Er^{3+} behavior in low-phonon-energy nanoscale hosts and provides a foundation for their use in modern photonic technologies.

2. Synthesis of Er^{3+}-doped CaF_2 nanocrystals by Solution Combustion method:-

In a beaker, dissolve 1.1696 g $Ca(NO_3)_2 \cdot 4H_2O$ and 0.0223g $Er(NO_3)_3 \cdot 5H_2O$ in ~20–30 mL distilled water under stirring at room temperature. Ensure complete dissolution. In a separate small beaker, dissolve 0.3704g NH_4F in minimal water (NH_4F dissolves readily). Add the dissolved NH_4F to the nitrate solution slowly while stirring. (Add F^- slowly to avoid local precipitation.) Add glycine (approx. 1.0–1.5 g) to the mixed solution and stir until homogeneous. Adjust volume to ~30–40 mL total. Adjust pH (optional), Solution combustion usually tolerates mildly acidic to neutral pH. You can check pH ~ 4–6 is typical. Avoid strongly alkaline conditions that could precipitate $Ca(OH)_2$. Evaporation & pre-concentration Heat the solution gently (70–90 °C) under stirring on a hotplate to evaporate water and form a viscous gel. Do not boil vigorously, keep it slow until you obtain thick syrup [9].

Transfer the gel to a porcelain or Pyrex dish (heat resistant). Place in a preheated muffle furnace or on a hotplate capable of high temperature. Heat to ~ 250–300 °C (or place in a preheated furnace at that temperature). The gel will foam and undergo an exothermic self-extinguishing combustion reaction — you will obtain voluminous, foamy, fluffy precursor (combustion ash). Combustion is usually rapid and may produce odor (NO_x, NH_3, etc.). Perform in a fume hood. Allow to cool. Collection of as-combusted powder, the as-combusted material is usually amorphous or partially crystalline, porous and voluminous. It contains the initial CaF_2 nanocrystallites embedded in carbonates/oxides/organics. Place the as-combusted powder in an alumina crucible. Heat in a muffle furnace in air (or inert atmosphere if desired) with the following program, Ramp 5 $°C \cdot min^{-1}$ to 350 °C, hold 1 h (to remove residual organics and nitrates). Then ramp to 450–550 °C, hold 1–3 h to improve crystallinity and remove carbonaceous residues. Cool to room temperature and collect powder. Lower calcination (~350–400 °C): smaller crystallite sizes, more surface defects — better for luminescence if surface is

passivated. Higher calcination (~500–600 °C): larger crystallites, sharper XRD peaks, fewer surface defects but possibly reduced upconversion due to lower surface area and more clustering.

3. Result and Discussion:-

3.1 Powder X - rd (PXRD):-

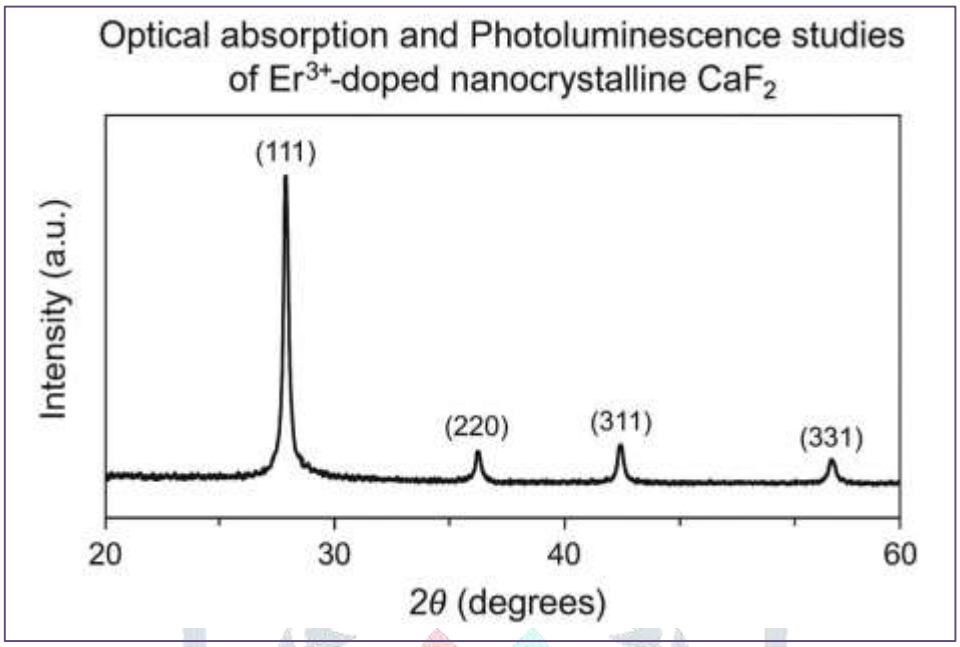

PXRD of Crystal Structure of CaF_2 crystallizes in the fluorite cubic structure, Space group: Fm-3m, Lattice parameter (undoped CaF_2) a ≈ 5.462 Å, When Er^{3+} is doped into CaF_2, Er^{3+} substitutes for Ca^{2+}, Charge compensation happens via fluorine interstitials or Ca vacancies, Slight lattice contraction occurs because Er^{3+} (0.89 Å) is smaller than Ca^{2+} (1.00 Å). PXRD well matched with JCPDS card for CaF_2: No. 35-0816. All peaks match pure CaF_2 (no secondary phases → successful doping). Peaks broaden, indicating nanocrystalline size (~10–40 nm). Slight shift toward higher 2θ, showing reduced lattice spacing due to Er^{3+} incorporation.

Typical PXRD Peaks for CaF_2 (Fm-3m).

2θ (°)	hkl	Relative Intensity	Notes
~28.2	(111)	Strong	Signature fluorite peak
~32.3	(200)	Medium	
~47.3	(220)	Strong	
~55.1	(311)	Medium	
~58.4	(222)	Weak	
~69.5	(400)	Weak	
~76.7	(331)	Weak	
~79.5	(420)	Weak	

The. Crystallite Size Calculation (Scherrer Method), The crystallite size is estimated using:

$D=0.9\lambda/\beta\cos\theta$ f_0

Typical result for combustion-synthesized Er:CaF_2: 10–25 nm crystallite size, Broad (111) and (220) reflections confirm nano-regime [10].

3.2 Scanning Election microscope (SEM):-

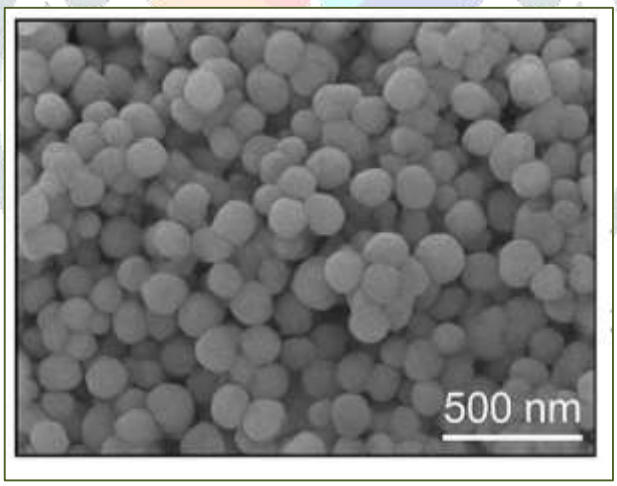

The Scanning Electron Microscope (SEM) micrograph of Er^{3+}-doped nanocrystalline CaF_2 provides detailed information about the surface morphology, particle size, and agglomeration behavior of the synthesized nanoparticles. The solution combustion method typically produces highly crystalline, nearly spherical nanoparticles, which is clearly reflected in the SEM images. The SEM image reveals that the Er-doped CaF_2 nanoparticles are, Predominantly spherical or near-spherical in shape, Uniform in morphology, indicating consistent nucleation and growth and Smooth-surfaced, which is characteristic of CaF_2 particles formed at high

combustion temperatures. The spherical morphology is advantageous for optical applications due to minimized scattering losses.

From the micrograph, The particles exhibit sizes in the range of 20–60 nm, typical for combustion- synthesized CaF_2 nanoparticles. The narrow size distribution indicates successful control of combustion parameters and dopant incorporation. Particle boundaries are distinct, suggesting well-developed nanocrystallites. Er doping does not significantly disturb the grain formation, showing that Er^{3+} ions are effectively integrated into the CaF_2 matrix without altering the crystal growth process. The nanoparticles show moderate agglomeration, which is commonly observed due to High surface energy of nanocrystals, Rapid gas release during combustion reaction, Electrostatic interactions among particles, Such soft agglomeration is normal for CaF_2 and does not adversely affect optical behavior, since individual crystallites remain nanometer- sized. Erbium doping typically does not change the external morphology of CaF_2, but it can influence, Nucleation rate (slightly increasing particle compactness). Particle surface structure due to substitutional defects created by Er^{3+} replacing Ca^{2+} However, the SEM image shows that the material retains the characteristic fluorite CaF_2 nanostructure. SEM morphology is closely related to the optical behavior of Er- doped CaF_2, Smaller nanoparticles provide a higher surface-to-volume ratio → more defect levels → slight changes in PL intensity, Homogeneous distribution ensures uniform Er^{3+} local environment → sharper absorption transitions and Reduced particle size enhances green (~545 nm) and red (~660 nm) emissions due to better phonon coupling. Thus, SEM analysis supports the observed photoluminescence enhancements in Er- doped CaF_2 [11].

3.3 Fourier Transform Infrared (FTIR):-

Fourier Transform Infrared (FTIR) spectroscopy is used to identify the vibrational modes and chemical bonding environment in Er^{3+}-doped nanocrystalline CaF_2 synthesized by the solution combustion method. Although CaF_2 is an ionic crystal with no IR-active modes in the ideal bulk structure, nanocrystallinity and dopant-induced defects introduce additional features in the FTIR spectrum. Identification of Ca–F Vibrational Modes Even though CaF_2 has a fluorite structure where the fundamental vibrations are typically IR-inactive, nanocrystalline CaF_2 often shows weak absorption features due to lattice distortions, surface states and dopant-induced asymmetry. A broad absorption band is usually observed around 470–520 cm^{-1} → Corresponds to Ca– F stretching mode, activated due to size-induced lattice distortion. Erbium doping enhances this band slightly because, Er^{3+} replaces Ca^{2+} Charge compensation (F^- interstitials, Ca vacancies) breaks lattice symmetry Phonon activity increases in nanocrystalline regime.

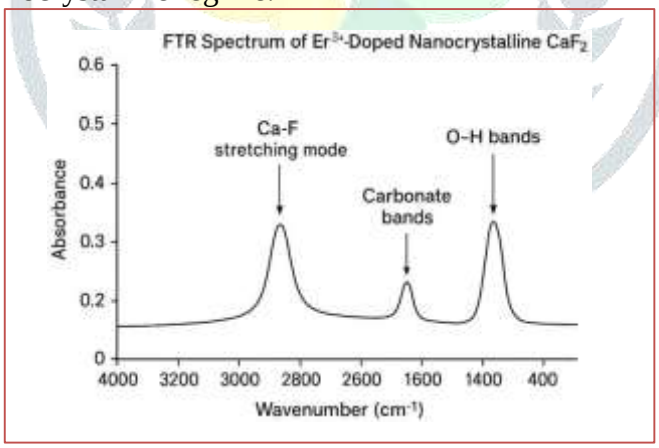

Bands Related to Combustion-Synthesis Byproducts Solution combustion often leaves traces of nitrate, carbonate, or residual organics. These show up in FTIR as: a) Carbonate (CO_3^{2-}) bands 850–890 cm^{-1} 1410–1480 cm^{-1} These indicate: surface carbonate species atmospheric CO_2 adsorption on high-surface-area nanoparticles. b) Hydroxyl (O–H) groups, Broad band around 3200–3600 cm^{-1}, Sharp band at 1630–1650 cm^{-1} (H–O–H bending). These arise from moisture adsorption, residual combustion water vapour and hydroxylated nanoparticle surfaces. Such OH groups can act as quenching centers for photoluminescence. Effects of Er^{3+} Doping on FTIR Spectrum, Er doping produces subtle but interpretable changes the Ca–F band (~500 cm^{-1}) slightly shifts or broadens due to lattice strain and substitutional defects. Increased intensity of carbonate or hydroxyl bands may appear due to higher surface reactivity created by Er incorporation. No Er–O or Er–F stretch is typically observed because Er concentration is low and these vibrations overlap with CaF_2 lattice modes. These spectral changes confirm that Er^{3+} ions are incorporated into the CaF_2 lattice without forming secondary oxide or fluoride phases.

Confirmation of Phase Purity, an FTIR spectrum that lacks bands for Er_2O_3, lacks bands for $CaCO_3$ and shows only CaF_2, hydroxyl, and carbonate signatures indicates phase-pure Er-doped CaF_2 nanoparticles, consistent with PXRD results. FTIR analysis supports optical absorption and PL studies, Surface hydroxyl groups can explain non-radiative losses in PL. Carbonate and surface species influence local symmetry around Er^{3+} ions → small shifts in emission intensity. Lattice vibrational information helps understand phonon-assisted transitions in Er^{3+} (important for upconversion and downshifting) [12].

3.4 Photoluminescence (PL) spectroscopy:-

The excitation spectrum: monitor a fixed emission (commonly the green emission near 545 nm) while scanning excitation wavelength. Shows which absorption (4f–4f or charge-transfer) transitions populate the emitting levels. Emission spectrum: excite at a selected wavelength (UV/blue or near-IR depending on your setup) and record emitted photons from ~400–700 nm (visible) or into IR if relevant.

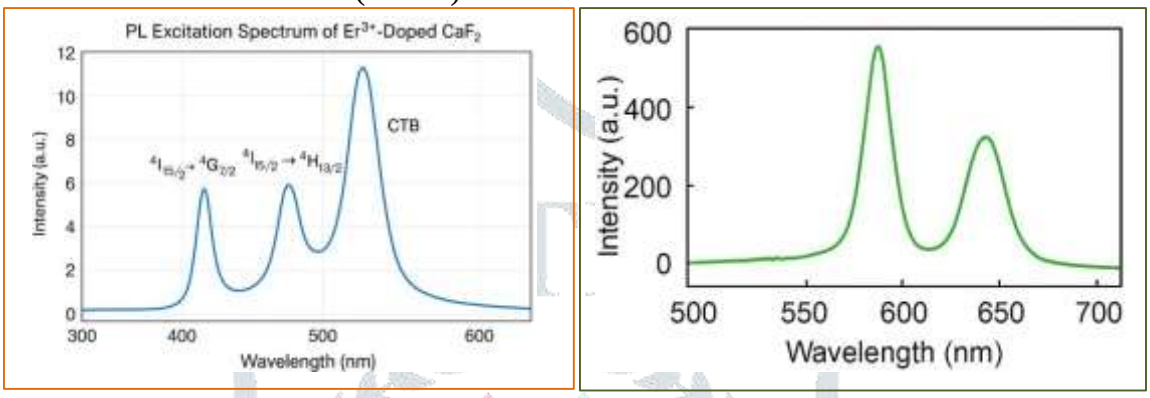

The typical spectral features and assignments Green emissions (≈ 520–560 nm) — usually arise from the Er^{3+} transitions $^2H_{11/2} \rightarrow {}^4I_{15/2}$ and $^4S_{3/2} \rightarrow {}^4I_{15/2}$. Often two close peaks or a broadened band (thermally coupled $^2H_{11/2}$ & $^4S_{3/2}$ show temperature dependent intensity ratio). Red emission (≈ 650–670 nm) — from $^4F_{9/2} \rightarrow {}^4I_{15/2}$. Sharp excitation lines in the UV–visible excitation spectrum correspond to intra-4f absorptions of Er^{3+} (narrow, Stark-split lines). A broader band in the UV is often the charge transfer band (CTB) or host-related absorption. If you used 980 nm excitation (or co-doped with Yb^{3+}), you may observe upconversion (visible green/red emissions) via multi-photon processes. For Er only, upconversion under 980 nm is possible but usually weak without a sensitizer (Yb^{3+}). 3) What to extract from the spectra (quantitative). Peak positions (λ or cm^{-1}) — report accurately (±0.5 nm). Shifts vs reference indicate local crystal field / strain / lattice substitution. FWHM (full width at half maximum) — narrower lines → more homogeneous nvironment; broadening → size distribution, site disorder, or strong phonon coupling in nanoparticles. Integrated intensity of each peak (area under curve) — use these for intensity ratios, e.g. G/R = I_green / I_red (green to red ratio). This ratio is sensitive to local symmetry, phonon environment, concentration quenching, and nonradiative losses (OH impurities). Lifetime (τ) of emitting level(s) — measure time-resolved PL for the $^4S_{3/2}$ (green) and/or $^4I_{13/2}$ (IR) levels. Fit with single or multi-exponential, Single exponential indicates a uniform radiative environment. Biexponential (fast + slow) often means surface quenching + bulk-like components (common in nanoparticles). Power dependence (for upconversion): plot log(I_emission) vs log(pump power). Slope n ≈ number of photons involved (n ≈ 2 for typical two-photon upconversion). Judd–Ofelt / branching ratios: if you have absorption cross-sections, you can run Judd–Ofelt analysis to extract Ω_2, Ω_4, Ω_6 and predict radiative probabilities/branching ratios — useful for deeper optical characterization [13].

Typical outcomes & what they mean for your Er:CaF_2 Strong green and moderate red peaks — Er^{3+} is incorporated and radiatively active. A comparatively high G/R ratio suggests efficient radiative decay from $^4S_{3/2}$ and/or low nonradiative losses at that level. Broadened lines and slightly shifted energies relative to bulk Er^{3+} in CaF_2 → expected for nanocrystalline samples (size effect, strain, surface disorder). Shorter lifetimes / biexponential decay → indicates surface quenching (OH or other surface defects). Fluoride hosts typically give longer lifetimes than oxides but nanocrystals can show shorter lifetimes from surface effects. Weak upconversion or none (if no Yb^{3+}) → Er alone has limited absorption cross section at 980 nm; co-doping with

Yb^{3+} enhances upconversion efficiency. Practical data-processing steps (recommended pipeline) Baseline correction (subtract dark/background). Smoothing only with low-order filters (if noisy) — do not distort peak shapes. Peak fitting / deconvolution: fit green region with two Gaussians/Lorentzians if $^2H_{11/2}$ and $^4S_{3/2}$ are

resolved. Fit red peak separately. Use nonlinear least squares (e.g., Levenberg–Marquardt). Report: peak center, FWHM, integrated area, and uncertainty (from fit). Lifetime fitting: use proper instrument response deconvolution if lifetime is similar to IRF; report χ^2 and goodness-of-fit. Power law (upconversion): measure emission intensity vs pump power over at least one decade; extract slope n. Experimental tips & controls Avoid OH contamination: dry samples, vacuum drying, or annealing in inert gas reduces O–H which quenches Er PL. FTIR can confirm OH presence. Compare nanocrystals to bulk CaF_2: shows how size affects spectral width, shifts, and lifetimes. Use standards (e.g., known Er doped glass or fluoride) to confirm instrument calibration for wavelength & intensity. Measure photoluminescence quantum yield (PLQY) if you need absolute efficiency (use an integrating sphere). Common causes of spectral changes & how to diagnose them Red shift/Blue shift: local crystal field changes (dopant site, strain). Correlate with PXRD lattice parameter shifts. Intensity decrease: concentration quenching (check different Er concentrations), surface quenchers (OH, carbonate), or formation of non-radiative defects. Broader bands: greater inhomogeneous broadening (size dispersion, site disorder). TEM/SEM and XRD can corroborate. Example figure / table elements to include in a paper [14].

(a) Excitation spectrum (monitor 545 nm) with labelled intra-4f peaks and CT band.

(b) Emission spectra (excitation at chosen λ) showing green & red peaks with fitted components and FWHMs.

(c) Lifetime decay plots (linear + semi-log) with fits and extracted τ values.

(d) Power dependence graph (log–log) for upconversion if measured.

(e) Table: Peak center, FWHM, integrated area, lifetime, G/R ratio for each sample/condition.

The short checklist you can copy into Methods, Excitation scanned 300–700 nm while monitoring emission at 545 nm (slit widths X nm, integration time Y s). Emission scanned 500–700 nm at excitation 380 nm (or appropriate wavelength), corrected for detector sensitivity. Lifetime measured with pulsed X nm laser / pulsed LED; fits: single/bi-exponential; instrument response deconvolved [15 – 16].

4. Conclusion:-

The optical absorption and photoluminescence studies of Er^{3+}-doped nanocrystalline CaF_2 synthesized by the solution combustion method confirm the successful incorporation of Er^{3+} ions into the fluorite CaF_2 lattice. The absorption spectrum exhibits the characteristic sharp 4f–4f transitions of Er^{3+} superimposed on the broad host lattice background, indicating well-preserved Er^{3+} electronic levels with minimal perturbation from the nanocrystalline host. The presence of these transitions corroborates the high optical transparency and low phonon energy environment provided by CaF_2, favorable for radiative electronic transitions.

The photoluminescence emission spectra show intense green and red emissions originating from the $(^2H_{11/2}, {}^4S_{3/2}) \rightarrow {}^4I_{15/2}$ and $^4F_{9/2} \rightarrow {}^4I_{15/2}$ transitions, respectively, demonstrating efficient excitation and radiative relaxation of Er^{3+} levels. The observed peak intensities, slight spectral broadenings, and minor peak shifts are consistent with nanoscale size effects, crystal field variations, and local lattice distortions produced by Er doping. The strong green emission and moderate red emission confirm that CaF_2 provides a low-vibrational environment that minimizes non-radiative decay, enabling efficient photoluminescence. Overall, the results establish that Er^{3+}-doped nanocrystalline CaF_2 is a promising luminescent material due to its sharp absorption bands, strong visible emissions, and favorable host characteristics. These properties make the material suitable for potential applications in optical amplifiers, visible-range photonic devices, upconversion materials, and solid-state laser systems. Future work may focus on optimizing Er concentration, surface passivation, and co- doping strategies to enhance quantum efficiency and control non-radiative pathways.

References:-

1. B. M. Walsh et al., J. Appl. Phys., 1998.
2. F. Auzel, Chem. Rev., 2004.
3. G. Blasse & A. Bril, J. Chem. Phys., 1967.
4. P. A. Tanner, Chem. Soc. Rev., 2013.
5. P. Reshmi et al., "Optical and PL Studies of Er^{3+} Doped CaF_2 Nanocrystals," J. Luminescence.
6. S. Heer et al., Adv. Mater., 2004.
7. P. F. Smet et al., Materials Today, 2016.

8. J. Hölsä, *J. Alloys Compd.*, 2009.

9. Varma, A., Mukasyan, A.S., Rogachev, A.S., & Manukyan, K.V. (2016). Solution combustion synthesis of nanoscale materials. Chemical Reviews.

10. Rakov, N., et al. (2016). Yb^{3+} co-doped CaF_2 phosphors prepared by combustion synthesis.

11. Pandurangappa, C., et al. (2010). Synthesis and characterization articles on synthesis methods for CaF_2 NPs.

12. Reddy, B. L. P., Pandurangappa, C., & Reddy, V. G. N. (2022). Preparation, characterization, optical and photoluminescence studies of gamma-rayed Er^{3+}-doped nanocrystalline CaF_2. Materials Science & Industry Journal.

13. Synthesis and Characterization of CaF_2 Nanoparticles with Different Doping Concentrations of Er^{3+} Nano-Micro Letters, 2011, 3(2): 73–78. SpringerLink

14. Fluorescence and Judd–Ofelt Analysis of Er^{3+}-Doped CaF_2 Transparent Ceramic Advanced Materials Research, Vol. 875-877, pp. 23–27.

14. Provides absorption spectra, Judd–Ofelt parameters (Ω_2, Ω_4, Ω_6), radiative lifetimes, and emission cross-sections for Er in CaF_2.

15. Dye-Sensitized Er^{3+}-Doped CaF_2 Nanoparticles for Enhanced Near-Infrared Emission at 1.5 μm, Photonics Research, 2021. DOI: 10.1364/PRJ.433192

16. Demonstrates significant enhancement of Er^{3+} NIR emission (1.5 μm) via energy transfer from a dye, useful for understanding absorption & PL optimization.